Low temperature conductivity in ferromagnetic manganite thin films: quantum corrections and inter-granular transport

2009 J. Phys.: Condens. Matter 21 186004

(http://iopscience.iop.org/0953-8984/21/18/186004)

J. Phys.: Condens. Matter **21** (2009) 186004 (8pp) doi:10.1088/0953-8984/21/18/186004

Low temperature conductivity in ferromagnetic manganite thin films: quantum corrections and inter-granular transport

Soumik Mukhopadhyay and I Das

ECMP Division, Saha Institute of Nuclear Physics, 1/AF, Bidhannagar, Kolkata 700064, India

E-mail: soumik.mukhopadhyay@saha.ac.in

Received 9 December 2008, in final form 3 March 2009
Published 6 April 2009
Online at stacks.iop.org/JPhysCM/21/186004

Abstract

The interplay between inter-granular transport and quantum corrections to low temperature transport properties of $La_{0.67}Sr_{0.33}MnO_3$ (LSMO) and $Nd_{0.67}Sr_{0.33}MnO_3$ (NSMO) thin films has been discussed. All the samples exhibit characteristics of renormalized electron–electron interaction in two dimensions. The contrasting response of the low temperature transport to magnetic field in the LSMO and NSMO films is attributed to the strikingly different magnetic field sensitivity of the inter-granular transport.

(Some figures in this article are in colour only in the electronic version)

1. Introduction

At low temperature, the resistivity of a ferromagnetic metallic manganite [1] undergoes an upturn resulting in a shallow minimum [2–5]. The observed resistivity minimum is explained by either introducing the concept of quantum corrections to conductivity (QCC) [3] or the extrinsic effect of grain boundaries [4–6]. Generally, one should be careful when using the quantum corrections for polycrystalline samples, since the grain boundary effects might mask the weak quantum contributions to low temperature resistivity [7]. However, very recently, a quantum interference effect characteristic of two-dimensional systems has been observed [8] in Fe and Ni polycrystalline films in the thickness range 3–300 nm, having grain sizes of a few nanometers. Hence there must be some criteria which allow QCC to manifest itself even in a granular system. In this paper, we will demonstrate that ferromagnetic manganite thin films of LSMO and NSMO having granular microstructures exhibit characteristics of QCC in two-dimensional systems. The sensitivity of the inter-granular transport to magnetic field in LSMO films being much higher compared to the NSMO film, the manifestations of QCC are more distinct in NSMO films.

The so-called quantum-mechanical corrections to low temperature conductivity [9] are: (1) the weak localization due to self-interference of coherently backscattered wavepackets and (2) the renormalized electron–electron interaction due to the diffusive motion of electrons in the presence of disorder potentials. In 2D systems both effects give rise to conductivity corrections proportional to $\log T$. In 3D systems, however, the correction factor is $T^{p/2}$, where $p = 1$ for interaction correction and $p = 2$–3 for localization contribution. Ideally speaking, a careful inspection of magnetoresistive properties should settle the issue [10]. The application of magnetic field should suppress the weak localization contribution, in that it destroys the phase coherence, thereby reducing the self-interference effect. Thus the dominance of weak localization should announce itself in negative magnetoresistance (MR) and the suppression of resistivity upturn in the presence of strong magnetic field. On the other hand, the renormalized electron–electron interaction leads to positive MR due to the spin-splitting effect [9].

Very recently the authors have presented a comprehensive description of spin-dependent transport in granular ferromagnetic manganites [4]. It was observed that the electric field dependence of conductivity at low temperature can be described by the functional form

$$G(\mathcal{E}) = G_0 \exp\left(\frac{-A}{\mathcal{E}}\right) \exp\left(\frac{\mathcal{E}}{\mathcal{E}_0}\right)^{1/2} \quad (1)$$

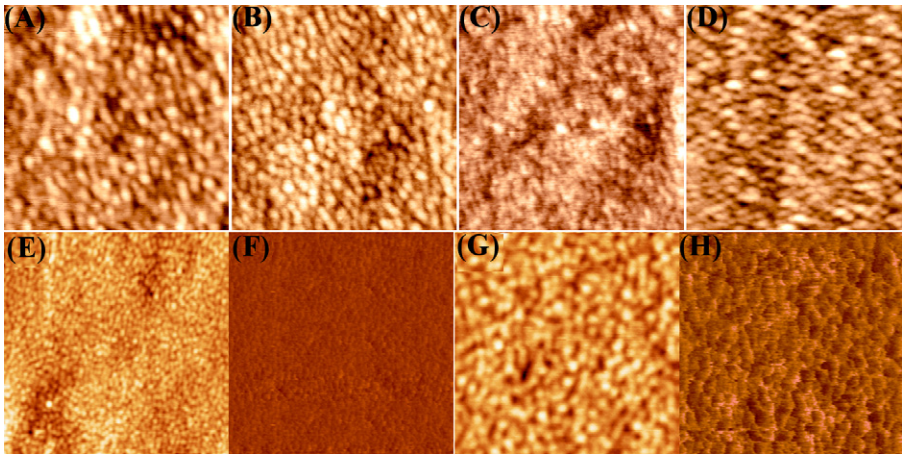

Figure 1. The AFM pictures over 500 × 500 nm^2 area for (A) LSTO1, (B) LSTO2, (C) LSTO3, (D) NSTO1; AFM and the corresponding MFM (frequency modulated) pictures for LSTO2 over ((E), (F)) 1 × 1 μm^2, ((G), (H)) 500 × 500 nm^2 (at room temperature).

G_0, A and $\mathcal{E}_0$ are the parameters for a given sample and the degree of their sensitivity to a magnetic field varies from sample to sample. The functional dependence was explained within a simple semiclassical treatment, a detailed description of which can be found in [4]. It considers a granular metallic system where each grain can be assimilated to localized sites at sufficiently low temperature. The electric field will affect two important parameters of the system: (1) the shape of the inter-grain potential barriers and hence the tunneling probability and (2) the energy E_a required for thermal activation over the potential barrier. The electrical conductance G_{ij} between sites i and j can be calculated from the total transport probability P_{ij}, which is the product of the tunneling probability across the barrier and the activation probability over the barrier. When the system under consideration is ferromagnetic, an additional factor must be taken into account, which is the inter-grain magnetic exchange. The magnetic exchange arises due to the spin conserved hopping from one grain to another. It will depend on the magnetic orientation and the overlap of electronic wavefunctions between nearest-neighboring grains. The relative contribution of inter-grain tunneling and non-tunneling transport comes out from the model calculation through the factor ξ_m, which is defined as the ratio of magnetic exchange energy and the total activation energy. The value of ξ_m can be estimated by fitting the conductance curves in the 'random' (in the absence of a magnetic field) and 'oriented' (in the presence of a magnetic field of a few kOe) configuration by equation (1) and expressing ξ_m in terms of the parameter $\mathcal{E}_0$ as $\xi_m = (\mathcal{E}_{0\uparrow\uparrow} - \mathcal{E}_{0\uparrow\downarrow})/(\mathcal{E}_{0\uparrow\uparrow} + \mathcal{E}_{0\uparrow\downarrow})$.

2. Experimental results and discussion

Thin films of $La_{0.67}Sr_{0.33}MnO_3$ (LSMO) having thicknesses 100, 50 and 25 nm each (designated as LSTO1, LSTO2 and LSTO3, respectively) and another film of $Nd_{0.67}Sr_{0.33}MnO_3$ (NSMO) having 100 nm thickness (NSTO1) were deposited on single-crystalline $SrTiO_3$ substrates using the pulsed-laser ablation technique. NSMO films of lower thickness were not considered since, being a narrow bandwidth system, they are susceptible to spatial phase separation between ferromagnetic metal and anti-ferromagnetic charge-ordered regions as the thickness is decreased (the biaxial strain due to film–substrate lattice mismatch is responsible for such phase separation [11]). All the films were deposited under identical conditions; the substrate temperature was 800 °C and the oxygen pressure 350 mTorr. The magnetic characterization was done using a commercial Quantum Design SQUID magnetometer and the ferromagnetic transition temperature for the as-prepared LSMO films turns out to be around 350–360 K while that for the NSMO film is about 220 K. The magnetotransport properties were studied using the standard four-probe method with the magnetic field applied parallel to the electric field. The surface morphology was analyzed using atomic force microscopy (AFM) and the magnetic imaging was done using magnetic force microscopy (MFM) in the frequency modulated mode. The AFM pictures show granular surface morphology and the average roughness for all the films turns out to be in the range 0.4–0.7 nm. A similar granular microstructure for manganite thin films has been reported elsewhere, too [12]. The MFM pictures show that magnetic domains exist even at room temperature (figure 1).

In figure 2, the resistivity of all the samples with the corresponding minimum value subtracted in the absence of, as well as in the presence of, a strong magnetic field has been plotted as a function of the square root of temperature (T). The linear fit to $\Delta\rho$ versus $T^{1/2}$ curve below the minima for all the samples is far from satisfactory. For LSMO films, the position of the resistivity minima shifts towards higher temperature with decreasing thickness, albeit marginally, and the enhancement in resistivity gets more pronounced as the thickness of the film is reduced. The NSMO film of thickness 100 nm exhibits a resistivity minima at a distinctly higher temperature compared to all the LSMO films. Application of a strong magnetic field brings out a contrasting response to resistivity so far as the LSMO films and the NSMO film are concerned. On the one hand, there is no perceptible change either in the position of the minima (T_m) or in the enhancement of resistivity below the minima for the LSMO films at strong magnetic field, while the

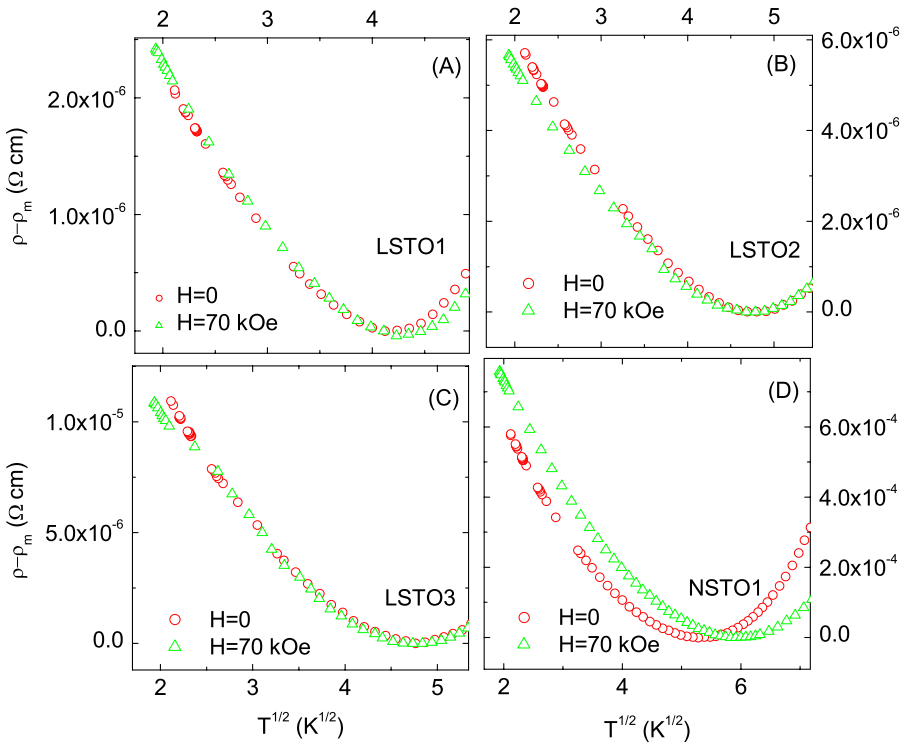

Figure 2. The resistivity after the subtraction of the corresponding minimum value is plotted against $T^{1/2}$ in the absence of magnetic field and in presence of strong magnetic field of 70 kOe for LSTO1 (A), LSTO2 (B), LSTO3 (C) and NSTO1 (D). It is evident that, for NSTO1, the minima is shifted to higher temperature and the upturn is enhanced at strong magnetic field.

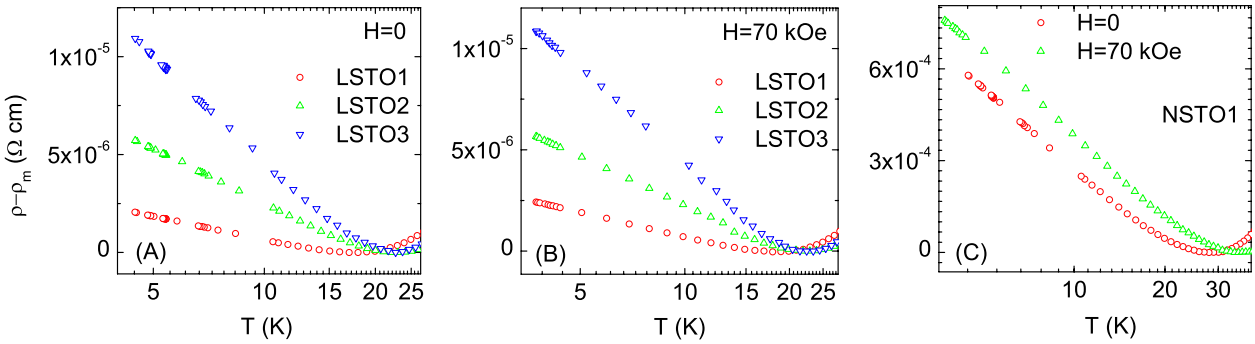

Figure 3. The temperature dependence of resistivity for LSTO1, LSTO2 and LSTO3 below the minima in the absence (A) and in the presence of magnetic field (B) showing clear logarithmic temperature dependence. (C) The temperature dependence of resistivity for NSTO1 below the minima in the absence and in the presence of magnetic field also showing log T behavior.

application of the same leads to a distinct shift of resistivity minima towards higher temperature along with an enhanced upturn of resistivity for the NSMO film. This is a clear signature of the dominance of renormalized e–e interaction [3] (the presence of weak localization would have led to the opposite phenomenon). It turns out that a resistivity correction for all the samples, in the absence of, as well as in the presence of, a strong magnetic field, gives a distinct $\Delta\rho \sim -\log T$ dependence (figure 3). Figure 4 clearly shows that $\log T$ is a better fit to the resistivity correction below the minima as compared to $T^{1/2}$. Apart from being the signature of the renormalized e–e interaction in 2D systems, such a temperature dependence is also typical of weak localization and the Kondo effect. A resistivity minimum due to the Kondo effect arises due to spin-flip scattering from magnetic impurities, which should be suppressed on application of a strong magnetic field. The shift of resistivity minima towards higher temperature with decreasing thickness for the LSMO films can be attributed to the enhanced scattering at the surface as the thickness is decreased [8].

As discussed earlier, both weak localization and the interaction effect give rise to logarithmic anomalies in resistivity. The cutoff length scale for electron–electron interaction is the thermal diffusion length given by $l_T = \sqrt{D\hbar/KT}$. The diffusion constant D can be calculated from the relation $D = \sigma_0/[e^2N(E_F)]$ using the value $N(E_F) = 2.4 \times 10^{22}$ eV^{-1} cm^{-3} for LSMO [13] and $N(E_F) = 3 \times 10^{18}$ eV cm^3 for NSMO [14]. The e–e interaction correction

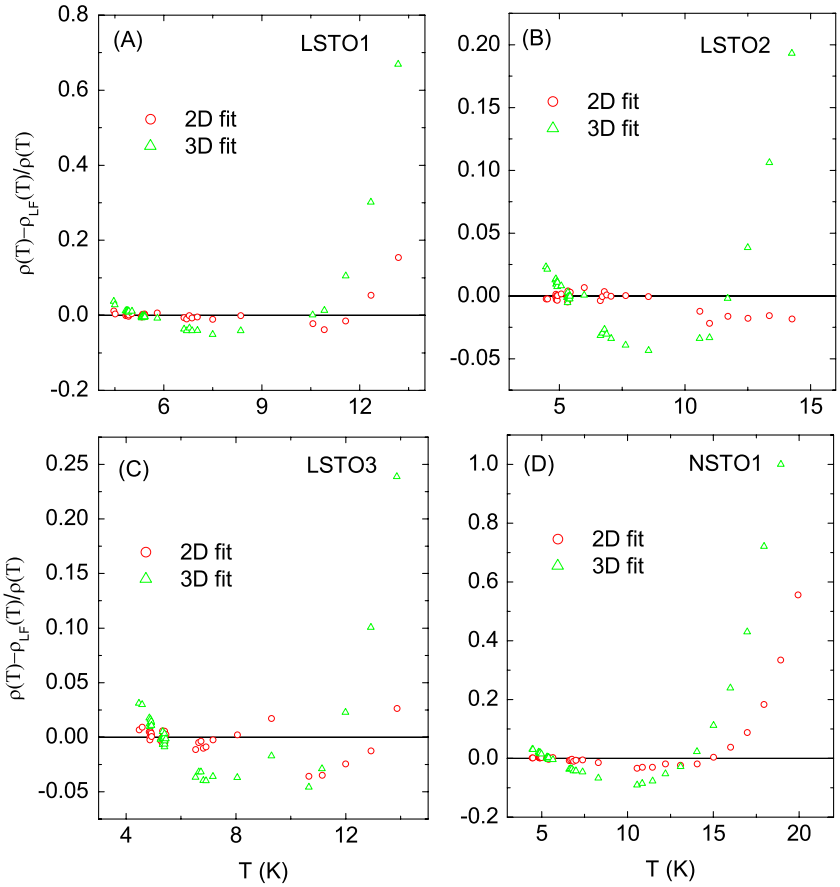

Figure 4. The normalized difference between the linear fit and the experimental data for both 2D and 3D cases, plotted against the temperature, shows that the linear fit for the 2D case is distinctly better than the 3D case.

in 2D, in the absence of a magnetic field, is given by [9],

$$\delta\sigma(0)_{\rm ee} = \frac{e^2}{4\pi^2\hbar}\left(2 - \frac{3}{2}\tilde{F_\sigma}\right)\log(T\tau_{\rm e}). \tag{2}$$

Here, $\tilde{F_\sigma} = -4[1 - 2(1 + F/2)\ln(1 + F/2)/F]$, where F is the screening factor in 2D and can be calculated by introducing the Thomas–Fermi approximation from the following expression [15]:

$$F = \frac{1}{\sqrt{1-x^2}}\left[1 - \frac{2}{\pi}\tan^{-1}\frac{x}{\sqrt{1-x^2}}\right]. \tag{3}$$

Here, $x = 2k_{\rm F}/\kappa$; the inverse screening length is given by $\kappa = e^2N_0/2\epsilon\epsilon_0$ ($\epsilon = 10$ for LSMO, $\epsilon = 20$ for NSMO and ϵ_0 being the vacuum permittivity). It turns out that the factor x is very small ($\ll 1$) and can be neglected in comparison to 1. Using this approximation, the screening factor F is estimated to be ~ 1 for all the samples, which gives $\tilde{F_\sigma} = 0.86$. Assuming that the boundary scattering is the basic elastic scattering mechanism (i.e. the elastic scattering length $l_{\rm e} \sim t$, the film thickness), the elastic scattering time $\tau_{\rm e}$ can be calculated. The magnetic field correction is given by [9]

$$\delta\sigma(H)_{\rm ee} = -\frac{e^2}{4\pi^2\hbar}g_2(h) \tag{4}$$

where $g_2(h)$ is a function of $h = g\mu_{\rm B}H/K_{\rm B}T$ which can be computed numerically [9]. Around 5 K and at a magnetic field of 7 T, $g_2(h)$ should be about 0.4.

The characteristic length scale for weak localization is the inelastic scattering length or the dephasing length $l_\phi = \sqrt{D\tau_\phi}$. The dephasing time τ_ϕ in 2D, when electron–electron scattering is the phase-breaking mechanism, is given by [16],

$$\tau_\phi{}^{-1} = \frac{KT}{2\pi N_0 D\hbar^2}\log(\pi D N_0\hbar) \tag{5}$$

where N_0 is the 2D density of states, which is $\sim 10^{18}$ eV^{-1} cm^{-2} for LSMO, estimated from the Hall effect measurement data [17] (for NSMO, N_0 was assumed to be $\sim 10^{14}$ eV^{-1} cm^{-2}). In the absence of a magnetic field, the correction term due to weak localization is [18],

$$\delta\sigma(0)_{\rm wl} = \frac{e^2}{2\pi^2\hbar}\log\left(2\frac{l_\phi^2}{l_{\rm e}^2} + 1\right). \tag{6}$$

The magnetic field correction to the weak localization contribution or the magnetoconductivity due to weak localization is given by [19],

$$\delta\sigma(B)_{\rm wl} = \frac{e^2}{2\pi^2\hbar}\left[\psi\left(\frac{1}{2} + \frac{\hbar}{4eBl_\phi^2}\right) - \psi\left(\frac{1}{2} + \frac{\hbar}{4eBl_{\rm e}^2}\right)\right] + \frac{e^2}{2\pi^2\hbar}\log\left(2\frac{l_\phi^2}{l_{\rm e}^2}\right). \tag{7}$$

Table 1. The weak localization and e–e interaction contributions to conductivity along with corresponding magnetic field corrections for all the samples.

Sample	ρ_m ($\mu\Omega$ cm)	T_m (K)	D (cm^2 s^{-1})	τ_e (10^{-11} s)	l_T (nm)	τ_ϕ (10^{-10} s)	l_ϕ (nm)	$\frac{\delta\sigma_{wl}}{\delta\sigma_{ee}}$	$\frac{\delta\sigma(7T)_{wl}}{\delta\sigma(0)_{wl}}$	$\frac{\delta\sigma(7T)_{ee}}{\delta\sigma(0)_{ee}}$
LSTO1	208	17	1.25	8	13	8.6	328	2	+0.98	−0.12
LSTO2	250	22	1.042	2.4	12	7.4	278	4	+0.97	−0.17
LSTO3	410	23	0.635	0.98	9	4.8	175	6.5	+0.92	−0.24
NSTO1	5116	28	407	0.025	231	0.5	1427	10	+1	−0.3

Here ψ is the digamma function, $\psi(z) = \frac{d}{dz}[\log\Gamma(z)]$. Some of the important physical quantities regarding the weak localization and interaction correction are given in table 1.

There are a few points to be noted here: (1) the thermal diffusion length l_T, which determines the dimensionality of the interaction correction, is much less than the thickness of the LSMO films, while the dephasing length is greater than the thickness of the LSMO films, indicating that, while the weak localization correction has a 2D character, the interaction correction is of a 3D nature, a scenario theoretically allowed [9]. (2) For the NSMO film, however, both interaction and weak localization correction has a 3D character. (3) The weak localization and interaction correction are almost equally influential in the absence of a magnetic field, with the localization contribution increasing with decreasing thickness of the LSMO films. (4) The effect of magnetic field on the interaction correction increases with decreasing thickness while for weak localization, the situation is exactly the opposite.

However, these trends are based on theoretical calculations excluding the effect of internal field in a ferromagnetic system. The strong internal magnetic field should suppress the weak localization contribution [10] and, on the other hand, enhance the interaction correction. From table 1, it is clear that the magnetic field correction term is much stronger for weak localization compared to the interaction correction, which agrees with the presumption that the internal magnetic field should significantly suppress the weak localization correction. Thus the ratio of weak localization and interaction correction given in table 1 is largely inflated. For NSMO, where there is a distinct manifestation of the interaction correction, the calculated value of $\delta\sigma_{wl}/\delta\sigma_{ee}$ is much higher compared to the LSMO films (table 1). Therefore the effect of weak localization in LSMO films can be considered to be minimal. The discrepancy in the dimensionality of the interaction correction between LSMO and NSMO can be understood if we consider that the density of states is derived from specific heat measurement on a bulk sample of LSMO [13] and may differ from the actual value for a thin film [20]. Moreover, due to the e–e interaction there would be a depletion of density of states at the Fermi level resulting in a larger value of D and hence the calculated value of l_T is underestimated. On the other hand, for NSMO, the $N(E_F)$ has been calculated from transport measurement on a thin film [17]. The possibility of a 2D nature of the interaction correction in LSMO films gains further support from the fact that the logarithmic anomalies in resistivity persist even at a magnetic field as high as 70 kOe, where the weak localization correction is non-existent for all practical purposes.

The LSMO films exhibit negative MR throughout the magnetic field range, with enhanced negative MR at low field, while the NSMO film shows positive low field MR before switching over to negative MR at higher magnetic field (figure 5). An important question which still begs an answer is: if the interaction effect is dominant even in the LSMO films, why is it that there is no manifestation in the response of the resistivity curves to the application of magnetic field? The interaction effect should give rise to positive MR. How is it getting suppressed? For the NSMO film, however, the shift of resistivity minima towards higher temperature and the enhanced resistivity upturn at strong magnetic field suggest that there is a positive contribution to the total MR due to the interaction effect. We should remember that orbital effects can also give rise to positive MR. A rough estimation of orbital MR (MR_{orb}) is possible using the expression $MR_{orb} \sim (H/ne\rho_0)^2$, where n is the carrier density and ρ_0 is the residual resistivity. It turns out that the positive MR contribution due to the orbital effect is negligibly small $\sim 10^{-4}$% even at a high magnetic field of 10 T.

The electric field dependence of conductivity below the resistivity minima for all the samples can be described by equation (1) (figure 6). This means that the effect of grain boundaries cannot be ignored altogether. The transport across the grain boundaries (discussed earlier) gives rise to negative MR and suppression of resistivity upturn as elaborated in [5]. The scaling parameters for the LSMO films are very sensitive to magnetic field, in sharp contrast to the NSMO film. It follows that the value of the factor ξ_m is very high for the LSMO films compared to the NSMO film where ξ_m is almost negligible (table 2). A high value of ξ_m means that there is a substantial contribution of inter-grain tunneling conduction vis-à-vis the non-tunneling inter-grain transport. As a result, there is far less probability of spin-flipping in LSMO films compared to the case for NSMO where inter-grain non-tunneling transport dominates [4]. The magnetic nature of the grain boundaries cannot be ruled out. But this can be taken care of adequately by our model used to analyze inter-granular transport, where the magnetic exchange term has been incorporated in the expression for inter-grain potential barrier [4]. So any change in the barrier shape affected by a magnetic field due to the magnetic nature of the barrier can be described by our model.

Thus, although the interaction correction leads to an enhancement of resistivity upturn on application of a magnetic field, the high sensitivity of inter-granular transport to magnetic

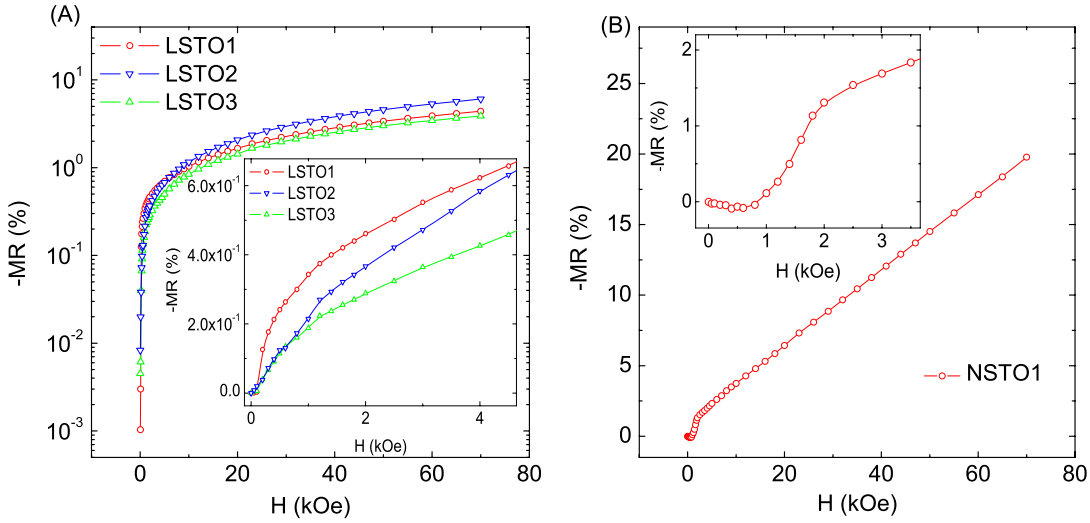

Figure 5. The magnetic field dependence of MR for (A) LSTO1, LSTO2, LSTO3 and (B) NSTO1 at 5 K. Insets: the blown-up portion around the low magnetic field region.

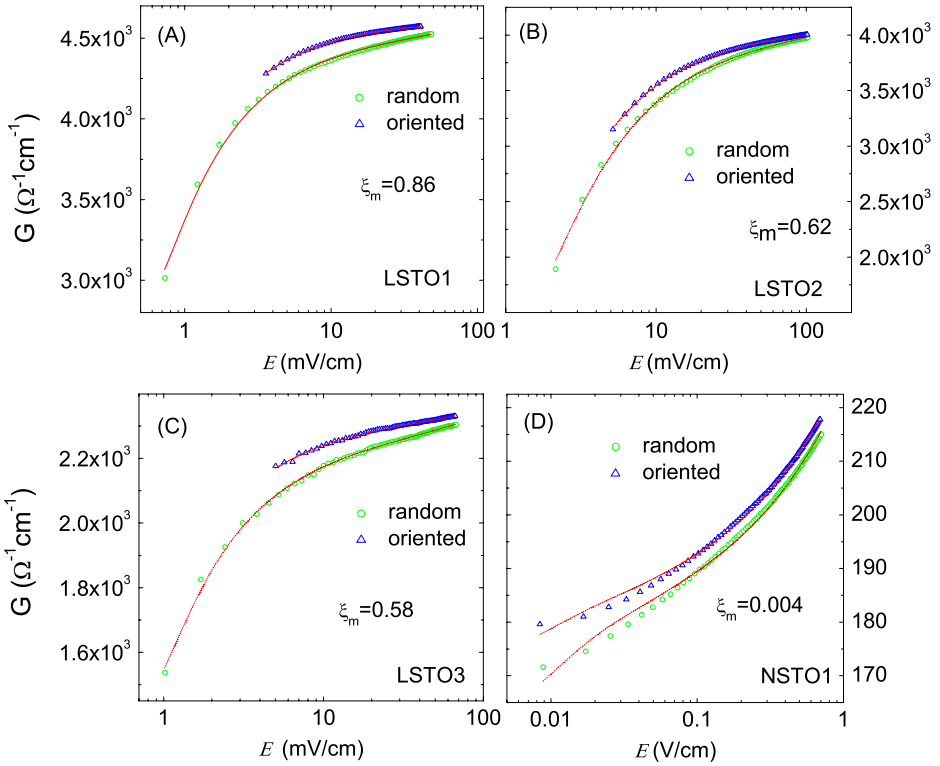

Figure 6. The electric field dependence of conductivity at 5 K, in 'random' ($H = 0$) and 'oriented' ($H = 5$ kOe) configuration fitted by equation (1) (shown by the continuous line) for (A) LSTO1, (B) LSTO2, (C) LSTO3 and (D) NSTO1.

Table 2. A few important parameters for the samples studied: $G_{0\uparrow\uparrow,\uparrow\downarrow}$, $\mathcal{E}_{0\uparrow\uparrow,\uparrow\downarrow}$ and $A_{0\uparrow\uparrow,\uparrow\downarrow}$ are the fitting parameters from equation (1) in the so-called 'oriented' and 'random' spin configuration, respectively.

Sample name	$G_{0\uparrow\uparrow}$ (Ω^{-1} cm^{-1})	$G_{0\uparrow\downarrow}$ (Ω^{-1} cm^{-1})	$\mathcal{E}_{0\uparrow\uparrow}$ (mV cm^{-1})	$\mathcal{E}_{0\uparrow\downarrow}$ (mV cm^{-1})	$A_{\uparrow\uparrow}$ (mV cm^{-1})	$A_{\uparrow\downarrow}$ (mV cm^{-1})	ξ_m
LSTO1	4572	4445	1.2×10^6	88 064	0.24	0.27	0.86
LSTO2	3968	3876	247 223	58 802	1.19	1.465	0.62
LSTO3	2287	2217	125 701	33 460	0.295	0.366	0.58
NSTO1	179	177	17903	17 767	2.6×10^{-4}	6×10^{-4}	0.004

field in the LSMO films (which leads to the suppression of the resistivity upturn) can mask the positive magnetoresistance due to the interaction effect. On the other hand, transport across the grain boundaries in the NSMO film is negligibly sensitive to the magnetic field, leaving the interaction correction to dominate the magnetotransport properties. Since the inter-granular transport is assumed to be elastic, the QCC effect showing two-dimensional behavior is quite plausible. The grains are well connected, unlike ceramic nanocomposites, and hence the spin disorder at the grain boundary should be thin enough (the domain walls look quite sharp even at room temperature as seen from the MFM picture in figure 1) to allow the electrons to be transmitted across the inter-grain potential barrier elastically. At strong magnetic field, the spin disorder is considerably reduced, resulting in the reduction of barrier width and hence the enhancement of conductivity or negative MR [21]. Although the sensitivity of inter-granular transport is comparatively much higher in LSMO films compared to the NSMO film, the negative MR at 7 T in NSMO is almost four times the value for the LSMO films. This large negative MR in NSMO, which has a much lower Curie temperature compared to LSMO, can be attributed to the suppression of spin fluctuation by magnetic field. There is a fundamental difference between the negative MR contributed by inter-granular transport and suppression of spin fluctuation. The inter-granular transport results in a low temperature resistivity upturn which can be partially suppressed by magnetic field, while, on the other hand, spin fluctuation and its response to a magnetic field have nothing to do with the resistivity upturn.

Moreover, the presence of spin–orbit scattering which leads to anti-localization and positive magnetoresistance (MR) [9] cannot be ignored altogether. The NSMO film exhibits small positive MR at very low magnetic field (inset, figure 5). Since the magnetic field correction to interaction effect which gives positive MR becomes dominant only at high magnetic field, the positive MR at such a low magnetic field is possibly due to spin–orbit scattering. We propose that the factor ξ_m being much greater in LSMO films, the negative low field MR due to the inter-granular transport is able to mask the positive MR at low field due to spin–orbit scattering. On the other hand, for NSMO, the factor ξ_m being very small, the spin–orbit scattering manifests itself in positive MR at low magnetic field.

It should be mentioned that Herranz *et al* [10] have reported QCC in metallic ferromagnetic $SrRuO_3$. Here, we have shown that the methodology employed there [10] for identifying the contribution due to QCC might be inconclusive in LSMO films because of the high sensitivity of its inter-granular transport to magnetic field. Rozenberg *et al* [6] observed a shallow resistivity minimum in polycrystalline manganites. The authors applied two models separately over the experimental data: (1) the inter-grain tunneling and (2) bulk scattering along with the QCC; and concluded that the inter-grain tunneling model qualitatively explains the data. On the other hand, Ziese [3] observed quantum interference effects in epitaxial LCMO films. However, no effort was made to delineate the grain boundary contribution. This paper does not merely deal with suppression of QCC due to grain boundaries; rather it focuses on the circumstances under which, even in the presence of grain boundaries, QCC can retain its influence. We have also emphasized the fact that it is not just the presence of grain boundaries which decides whether QCC will be manifested or suppressed; rather it is the sensitivity of inter-granular transport to magnetic field which is the more important factor.

There are recent papers suggesting the presence of electronic inhomogeneities at low temperature in ferromagnetic metallic manganites. For example, it has been observed that a sufficiently large biaxial strain can lead to electronic inhomogeneities even in a canonical double-exchange system such as LSMO [22]. However, in this case, the experiments have been carried out for LSMO films having thicknesses high enough so that the strain due to film–substrate lattice mismatch is relaxed and the influence of inhomogeneity is negligible. We have not observed any manifestations of inhomogeneity in the transport properties such as hysteresis in the magnetic field dependence of MR, long time relaxation, etc. Sagdeo *et al* attributed the low temperature minima in LCMO films [23] to electronic inhomogeneity (although stronger evidence of long time relaxation is lacking). However LCMO has a lower bandwidth compared to LSMO and hence should be prone to phase separation. It should also be noted that theoretically the resistivity of manganites has been studied using a random resistor network based on phase separation between metallic and insulating domains, which explains the metal–insulator transition (resistivity maxima) at high temperature without predicting any low temperature minima in resistivity [24].

3. Summary

The influence of grain boundaries and the quantum corrections on the magnetotransport properties of ferromagnetic manganite thin films has been investigated. It turns out that the manifestations of transport across the grain boundaries and quantum corrections can coexist. The conductivity correction exhibits $\Delta\sigma \sim \log T$ behavior in the absence of, as well as in the presence of, a magnetic field, which is a characteristic of renormalized e–e interaction in two dimensions (together with the fact that the resistivity minima remains independent of magnetic field or shifts towards higher temperature). The electric field dependence of conductivity at low temperature is given by $G(\mathcal{E}) = G_0 \exp(\frac{-A}{\mathcal{E}}) \exp(\frac{\mathcal{E}}{\mathcal{E}_0})^{1/2}$, which suggests that the effect of a combination of spin-dependent inter-grain tunneling and non-tunneling transport cannot be ignored either. The high sensitivity of inter-granular transport to magnetic field in LSMO films, on the one hand, and the lack of it in the NSMO film on the other, results in the more distinct manifestation of quantum corrections in the NSMO film compared to the LSMO films.

Acknowledgments

The authors would like to acknowledge P Mishra and D Ghosh of the Surface Physics Division, SINP, Kolkata for providing the AFM and MFM facilities.

References

[1] Tokura Y 2000 *Colossal Magnetoresistive Oxides* (Amsterdam: Gordon and Breach)
[2] Hwang H Y *et al* 1996 *Phys. Rev. Lett.* **77** 2041
[3] Ziese M 2003 *Phys. Rev.* B **68** 132411
[4] Mukhopadhyay S and Das I 2007 *Phys. Rev.* B **76** 094424
[5] Mukhopadhyay S and Das I 2007 *Europhys. Lett.* **79** 67002
[6] Rozenberg E, Auslender M and Felner I 2000 *J. Appl. Phys.* **88** 2578
[7] Rozenberg E and Auslender M I 2002 *J. Phys.: Condens. Matter* **14** 8755
[8] Gerber A *et al* 2007 *Phys. Rev. Lett.* **99** 027201
[9] Lee P and Ramakrishnan T V 1985 *Rev. Mod. Phys.* **57** 287
[10] Herranz G *et al* 2005 *Phys. Rev.* B **72** 014457
[11] Biswas A *et al* 2001 *Phys. Rev.* B **63** 184424
[12] Dey P, Nath T K and Taraphder A 2007 *Appl. Phys. Lett.* **91** 012511
[13] Woodfield B F, Wilson M L and Byers J M 1997 *Phys. Rev. Lett.* **78** 3201
[14] Banerjee A *et al* 2003 *Phys. Rev.* B **68** 186401
[15] Al'tshuler B L and Aronov A G 1985 *Electron–Electron Interaction in Disordered Systems* (Amsterdam: North-Holland)
[16] Al'tshuler B L, Aronov A G and Khmelnitskii D E 1982 *J. Phys. C: Solid State Phys.* **15** 7367
[17] Zhao K *et al* 2006 *Appl. Phys. Lett.* **88** 141914
[18] Beenakker C W J and van Houten H 1998 *Phys. Rev.* B **38** 3232
[19] Al'tshuler B L *et al* 1980 *Phys. Rev.* B **22** 5142
[20] Okawa N *et al* 2000 *Solid State Commun.* **114** 601
[21] Balcells L I *et al* 1998 *Phys. Rev.* B **58** R14697
[22] Mukhopadhyay S, Das I and Banerjee S 2009 *J. Phys.: Condens. Matter* **21** 026017
[23] Sagdeo P R *et al* 2008 arXiv:0804.4247v1[cond. mat.]
[24] Mayr M *et al* 2001 *Phys. Rev. Lett.* **86** 135